Adler synchronization of spatial laser solitons pinned by defects

P.V. Paulau[1], C. McIntyre[2], Y. Noblet[2], N. Radwell[2], W.J. Firth[2], P. Colet[3], T. Ackemann[2], and G.-L. Oppo[2]

[1] *TU Berlin, Institut für Theoretische Physik, Hardenbergstr. 36, Sekr EW 7-1, 10623 Berlin, Deutschland*
[2] *SUPA and Department of Physics, University of Strathclyde, 107 Rottenrow, Glasgow G4 0NG, UK and*
[3] *IFISC, (CSIC-UIB), Campus Universitat Illes Balears, E-07071 Palma de Mallorca, Spain*

Defects due to growth fluctuations in broad-area semiconductor lasers induce pinning and frequency shifts of spatial laser solitons. The effects of defects on the interaction of two solitons are considered in lasers with frequency-selective feedback both theoretically and experimentally. We demonstrate frequency and phase synchronization of paired laser solitons as their detuning is varied. In both theory and experiment the locking behavior is well described by the Adler model for the synchronization of coupled oscillators.

Spontaneous breaking of the translational symmetry in spatio-temporal systems leads to the formation of nonlinear structures such as patterns, solitons, oscillons, vortices and disorder [1]. Laser cavity solitons (LCS) are nonlinear self-localized dissipative states that possess both translational and phase invariance. The interaction of LCS leads to phase-locked bound states with well defined phases and separations as predicted for example in the cubic-quintic Complex Ginzburg Landau (CGL) equations for temporal solitons in mode-locked lasers [2–8] and in models of lasers with saturable absorbers for the spatial case [9–11]. Corresponding bound states have been observed experimentally in fiber lasers [12, 13].

Spatial LCS have recently been observed in semiconductor-based micro-resonators with either frequency-selective feedback [14, 15] or saturable absorption [16, 17]. For temporal LCS, such as those arising in fiber lasers, the effects of longitudinal inhomogeneities are washed out by the propagation dynamics along the cavity axis, and every soliton sees the same material characteristics. Spatial LCS in real systems are usually pinned by defects resulting from fluctuations during the epitaxial growth process [15, 18]. Besides fixing the position, these defects induce a shift in the LCS natural frequency. The frequency shift depends on the characteristics of the defect itself and typically is different for each of them. This diversity in natural frequencies is a critical ingredient for the description of spatial LCS in real systems. Therefore, despite being suitable for temporal LCS, theoretical studies considering the interaction of identical LCS arising on a homogeneous background are not adequate to describe the dynamics of coupled spatial LCS. Here we show that the interaction of pinned LCS with different intrinsic frequencies can be suitably described by the Adler locking mechanism [19]. In particular we show that the coupling, if strong enough, can overcome the natural disorder leading to a synchronous regime characterized by emission at a common frequency with a phase difference that has a precise dependence on the frequency difference. The Adler locking mechanism has relevance in biological

clocks, chemical reactions, mechanical and electrical oscillators [20]. In optics frequency locking of the Adler type was first observed in lasers with injected signals [21] with more recent generalizations to coupled lasers [22], the spatio-temporal domain [23], quantum dot lasers [24] and frequency without phase lockings [25].

We first present frequency locking and phase synchronization of spatial LCS pinned by defects in a general CGL model with frequency-selective feedback where spatial variations of the cavity tuning parameter are used to simulate the presence of background defects. To show universality, defect induced Adler synchronization is then demonstrated in a model closer to the experimental realization where the saturable carrier dynamics are included [26]. Finally, the phenomenon is demonstrated experimentally in a Vertical Cavity Surface Emitting Laser (VCSEL) with an external Bragg grating that provides frequency-selective feedback [15].

The interaction and locking phenomena which we observe in a semiconductor laser with feedback are well captured in a simple generic model consisting of a cubic CGL equation where solitons are stabilized by coupling to a linear filter equation [27]:

$$\partial_t E = g_0 E + g_2 |E|^2 E - i\partial_x^2 E + F + in(x)E,$$
$$\partial_t F = -\lambda F + \sigma E, \tag{1}$$

where $E(x)$ is the intra-cavity field and $F(x)$ is the filtered feedback field. Note that the linear feedback equation breaks the Galilean invariance of the cubic CGL equation. For clarity reasons, we focus here on one transverse spatial dimension. The time and space coordinates (t, x) are scaled to 1 ns and 40 μm, respectively, so that g_0, describing linear gain and detuning, and g_2, describing nonlinear gain and dispersion, are dimensionless. We consider pure diffraction which is appropriate for VCSEL systems. The real function $n(x)$ describes spatial variations of the cavity tuning due to background defects that predominantly perturb the material refractive index. In the second equation of (1) σ is the feedback strength, λ its bandwidth, and we have implicitly set our reference fre-

quency to the peak of the filter response. System (1) has exact solutions corresponding to stable single-frequency chirped-sech solitons [27]. Small variations of $n(x)$ lead to pinning and small changes in the soliton frequency. The interaction of spatially separated pinned solitons can lead to their locking which is our main interest here.

We consider parameter values given by: $g_0 = -4 + 28i$, $g_2 = -96 - 48i$, $\lambda = 2.71$, $\sigma = 162.6$, for which, in the ideal case with translational invariance, $n(x) = 0$, system (1) has stable solitons with two free parameters: location and phase. The interaction of two such solitons makes them spiral slowly to fixed relative distances L and a phase difference $\Phi = \phi_2 - \phi_1 = \pi/2$ unless merging takes place. Φ equal to zero and π are also possible but correspond to saddles that are either phase or distance unstable. Analytically the attainment of a bound state reduces to the analysis of two transcendental equations in the (L,Φ) phase space. The situation is very similar to that described in [3, 6, 9] for bound solitons.

We now consider the case where the interaction takes place between pinned solitons since the translational invariance is broken by the pinning potential $n(x)$ which is equal to zero everywhere except in the intervals $x_j - W < x < x_j + W$ where

$$n(x) = \frac{-n_j}{2} \left[cos \left(\frac{\pi(x - x_j)}{W} \right) + 1 \right] \qquad (2)$$

with $j = 1, 2$. The pinning potential is a smooth function of x and the width $2W$ of the defects is chosen to be close to the width at half maximum of the LCS to help a quick convergence of the soliton distance to the final defect separation. Differences between the defects are described by the depths n_1 and n_2 of the pinning potential. The values of n_j considered here preserve the structure of the LCS with only its frequency ω_j shifted.

If the defects are close enough in space, the soliton interaction locks their frequencies and phases to common values that depend on the difference between the defect depths. The synchronization dynamics of the phase difference Φ between the pinned solitons relaxes to well determined stationary values that depends on the defect detuning parameter $\Delta\omega = \omega_2 - \omega_1$ generated by the choice of n_1 and n_2 values. The dependence of the stationary phase difference Φ on the detuning $\Delta\omega$ for numerical simulations of (1) is shown in Fig. 1 for $|x_2 - x_1| = 1.5$ space units. There are a maximal and a minimal detuning $\pm\Delta\omega_{th}$ below and above which synchronization does not take place. Very similar results have been obtained from numerical simulations of LCS in models of VCSELs with frequency-selective feedback that include the dynamics of the carriers and more realistic values of the linewidth enhancement factor [26] (see Fig. 1).

The archetypical equation describing synchronization between two coupled oscillators is the Adler equation
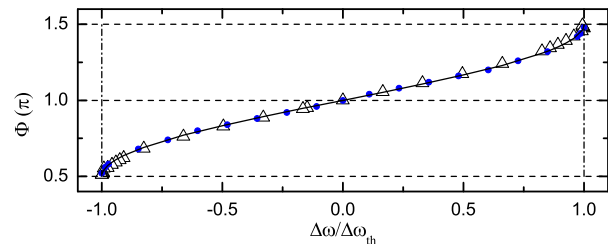

FIG. 1: (Color online) Locked phase differences Φ of pinned LCS for different frequency detunings (controlled by the potential depths n_1 and n_2) from direct integration of Eq. (1) (dots, LCS separation of 5.3 soliton widths) and the model of Ref. [26] (triangles, LCS separation of 4 soliton widths). The solid line refers to the Adler equation (3).

[19],

$$\frac{d\Phi}{dt} = \Delta\omega - \varepsilon \sin(\Phi), \qquad (3)$$

where in-phase and anti-phase solutions are selected for zero detuning, $\Delta\omega = 0$, depending on the sign of the coupling parameter ε: for positive ε the final stable state is $\Phi = 0$; for negative ε it is $\Phi = \pi$. A comparison of the results of the Adler equation with negative ε and the simulations of the synchronization of LCS in both equations (1) and the model of Ref. [26] is presented in Fig. 1. The agreement is remarkable. Note that the $\pi/2$ value observed in phase locking of dissipative solitons without defects [13] is now replaced by the π value typical of Adler synchronization. In-phase and out-of-phase values have already been observed in numerical simulations of LCS in cubic-quintic CGL equations with regular variations of the background [28, 29] although no Adler scenario is suggested. In particular unless the period of the modulation is much larger than the length scales due to soliton interaction, the LCS are forced into different minima of the potential and do not experience any detuning difference anymore [29]. This is consistent with the π-phase states we observed for localized defects of equal depths ($|n_2 - n_1| = 0$).

To characterize the Adler locking both in the spatial and temporal domains, we display the time averaged far field images in the top part of Fig. 2 and the optical spectra in bottom part of Fig. 2 for two points inside ($\Delta\omega/\Delta\omega_{th} = 0$ and 0.99) and one outside the Adler region ($\Delta\omega/\Delta\omega_{th} = 2$), respectively. Progressive change of the LCS phase difference Φ (from π in Fig. 2a to around 1.5π in Fig. 2b) is reflected in the change in the symmetry of the fringe pattern. Far field fringes are well defined in the region where the LCS are locked in frequency (see the full overlap of the soliton peaks in the frequency spectrum in Fig. 2d and 2e) indicating a strong interaction. For detunings much larger than the locking range, the fringe visibility disappears and the spectrum is formed

just by the lines of the individual solitons (not shown) corresponding to LCS operating independently. For detunings just outside the Adler locking region, however, some phase and spectral correlation survives due to non-uniform evolution of the relative phase (Figs. 2c and 2f).
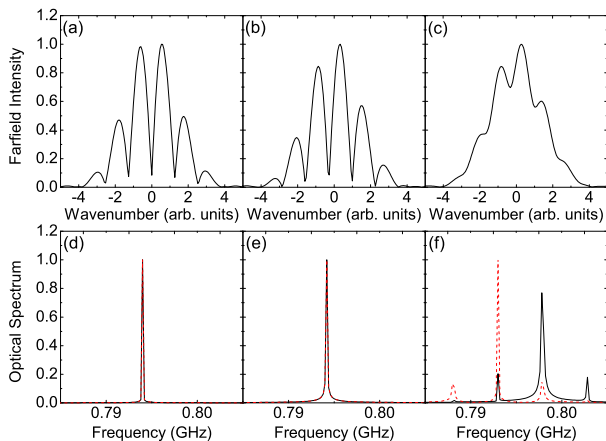

FIG. 2: (Color online) Far field fringes (a)-(c) averaged over 2 μs, and optical spectra (d)-(f) for a time window of 5 μs, for $\Delta\omega/\Delta\omega_{th} = 0$ (a,d), 0.99 (b,e) and 2.0 (c,f) obtained from simulations of the model of Ref. [26]. In (d,e) the LCS spectral peaks (dashed and solid lines) overlap.

The Adler locked state between LCS is a robust feature independent of initial conditions such as initial phases, frequencies and sequential order of creation of the two LCS. Once the locked state is attained, one of the two LCS can be switched off by a short, localized perturbation to the carrier density at its location. Hence, LCS retain their solitonic properties in the phase-locked state in the sense that they are still individually bistable and optically controllable.

The experiment has been performed with a temperature tuned 981 nm VCSEL of 200 μm circular aperture and a volume Bragg grating (VBG) with a single reflection peak at 981.1 nm, a reflection bandwidth of 0.2 nm full-width at half-maximum (FWHM) and a peak reflectivity of 99% [15]. The external cavity for the frequency-selective feedback is arranged in a self-imaging configuration that maintains the high Fresnel number of the VCSEL cavity and ensures local feedback compatible with self-localization (see Fig. 3). Small deviations from the self-imaging condition are not critical for the reported phenomena. The detection system comprises two charge-coupled-device cameras for near- and far-field imaging, and a scanning Fabry-Perot interferometer with a 10 GHz free spectral range to measure the optical spectrum. Several LCS appear at certain spatial locations defined by the traps when increasing the VCSEL injection current and display hysteretic behavior when decreasing the current again. The experiment described below is performed at a bias current at which both LCS involved are indi-

vidually bistable. Investigations were performed on pairs of different LCS with a distance of 30 to 80 μm. We focus here on a configuration of two LCS a distance of 79 μm, but the results are typical also for the other configurations. Each of these LCS is a coherent emitter but they are usually mutually incoherent due to the disorder [15, 18].
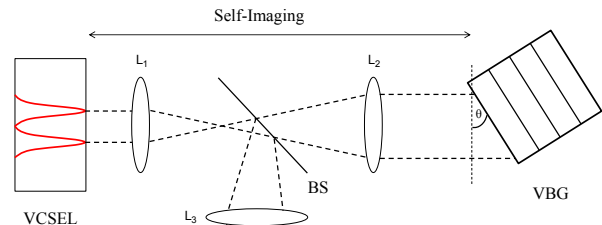

FIG. 3: Schematic diagram of a self-imaging cavity coupling a VCSEL to a frequency-selective element. The beam profiles indicate two interacting LCS. The dotted lines correspond to the centers of the bundle of rays emitted by the soliton. The tilt angle Θ is greatly exaggerated for clarity of display. The focal lengths of the intra-cavity lenses L_1, L_2 are $f_1 = 8$ mm and $f_2 = 50$ mm, the total cavity length $L \approx$ 12 cm with a 1.23 GHz free spectral range. L_3 images the near field of the VCSEL into the detection arm.

Since it is experimentally awkward to vary the detuning between two LCS by locally changing the properties of the VCSEL itself, we use a piezo-electric transducer to minutely tilt the external cavity's end reflector (VBG) with respect to the optical axis. This leads to a differential change of the external cavity length for the two LCS and thus to a differential change in feedback phase, which can be incorporated into Eqs. (1) by making σ complex. In this way the frequency difference, i.e. the detuning $\Delta\omega$, between two LCS can be tuned [30]. During the scan, LCS position in near field and angular center in far field stay constant to better than 5% and 2.5% of their width, respectively. When performing such a scan, a region of frequency and phase locking appears, identified in Fig. 4 by the region of high fringe visibility in the far field. These fringes are video integrated over a time of 20 ms (significantly longer than any intrinsic time scale) and last for seconds to hours depending on parameters. This illustrates that locking – once achieved by a careful alignment of the VBG – is a robust phenomenon.

As expected for the Adler scenario, in the locking region, the fringe phase varies smoothly and quasi-linearly with the detuning of the external cavity. It is much more noisy outside, where the visibility is low. There is no significant phase hysteresis when the tilting is reversed (see the green solid and dashed lines in Fig. 4), again as expected for the Adler scenario. The transitions to

and from frequency and phase-locking are rather abrupt (Fig. 4, black curve). For clarity, we show only a single sweep of the fringe visibility, because there is significant jitter at the transition points. This and the fact that the locking range is only about $\pi/2$ can be attributed to features beyond the phase-only approximation underlying the Adler equation such as the multi-longitudinal mode structure and possibly amplitude dynamics [31]. Longitudinal mode hopping of individual solitons can enable and/or quench the Adler dynamics thus explaining the jitter and limited locking range of (Fig. 4). Within the locked region, however, the dynamics follows the Adler scenario with the locking phase being determined by the solitons' differential feedback phase.

The importance of the external cavity structure is also evidenced by the fact that locking-unlocking scenarios can be induced by changing the VCSEL current if the VBG is adjusted close to the locking region. In this case the refractive index effects due to the ohmic heating shift the cavity resonances and induce hopping between different external cavity modes for each individual soliton. The LCS can then lock to a common external cavity mode for some range of the injection current and display again Adler interaction.
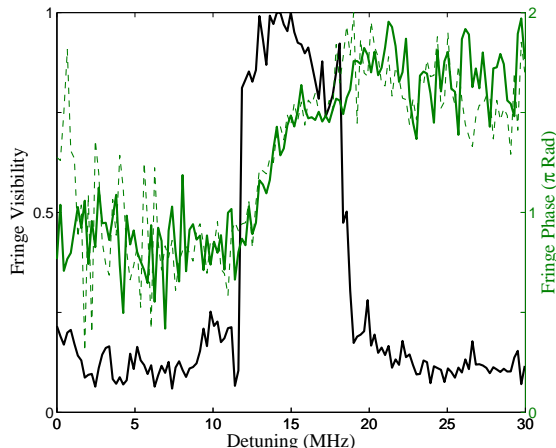

FIG. 4: (Color online) Fringe visibility (black) and fringe phase (green curves, gray in print) as a function of the tilt angle that changes the difference between the feedback phases of the LCS. This difference is converted to a frequency scale by multiplying it by the free spectral range of the external cavity thus providing the change of the relative detuning between the two LCS in the external cavity. The zero of this detuning scale is arbitrary. The solid and dashed green curves are obtained for scanning the tilt back and forth. The fringe phase is obtained from the phase of a cosine-wave fitted to far field profiles like those in the upper row of Fig. 5. Other parameters: Temperature $69°$C, current $I = 373$ mA.

Fig. 5 shows experimental far-field fringes (upper part) and the corresponding optical power spectra (lower part),

to be compared with the numerical results of Fig. 2. When the fringe visibility is high (Figs. 5a, b), the two LCS have the same frequency (Figs. 5d, e). Weak side-modes indicate some residual excitation of neighboring external cavity modes. The change in fringe phase from π (Fig. 5a) to $1.5\,\pi$ (Fig. 5b) is reflected in the change in symmetry of the fringe pattern. Outside the locking region the fringes essentially disappear (Fig. 5c) and the two LCS operate on different frequencies.
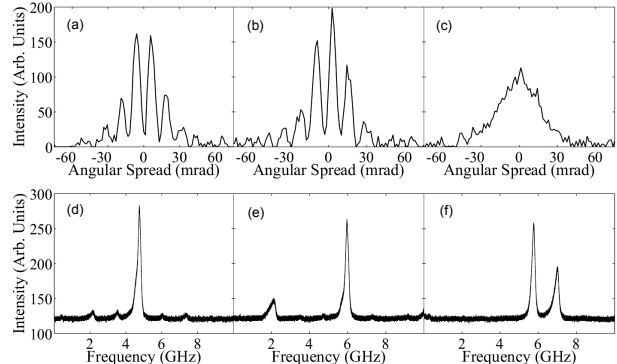

FIG. 5: Upper row: cut through far field intensity distribution orthogonal to fringe orientation. Lower row: optical power spectra. Left column (a,d) for detunings around 12 MHz, locked with a phase of π; center column (b,e) around 18 MHz, near the end of the locking region, locked with a phase of $1.5\,\pi$; right column (c,f) around 22 MHz, unlocked, no clear fringes.

Synchronization behavior has been discussed in both continuous and coupled oscillator models [20]. Our study uses a continuous model, but synchronization is between 'discrete' entities, the solitons. As such, self-localized solitonic oscillators provide a nice bridge between spatially extended media and coupled, pre-defined oscillators. Although we have demonstrated the validity of Adler's model for just two solitons, we suggest that network synchronization in the spirit of Kuramoto's model (with coupling possibly controlled by the deviation from the self-imaging condition) should be possible with many LCS in a fruitful analogy with brain activity [32] and, possibly, with spatio-temporal excitability [23].

In conclusion, we have demonstrated spatio-temporal Adler synchronization without injection in semiconductor lasers with frequency selective feedback. The synchronization is induced by spatial defects where the LCS are pinned. The presence of the defects breaks the translational symmetry, fixes the relative distance between solitons and locks the relative phase to values different from $\pi/2$ observed numerically in the absence of defects or experimentally in temporal-longitudinal systems. A regime of Adler synchronization is identified when changing the frequency of each soliton with respect to that of its neighbour.

[1] M. Cross and H. Greenside, *Pattern formation and dynamics in nonequilibrium systems*, (Cambridge University Press, Cambridge, 2009).

[2] B.A. Malomed, Phys. Rev. A **44**, 6954 (1991).

[3] N.N. Akhmediev, A. Ankiewicz, J.-M. Soto-Crespo, Phys. Rev. Lett. **79**, 4047 (1997).

[4] N. Akhmediev, F. Zen, P. Chu, Opt. Comm. **201**, 217 (2002).

[5] H. Leblond, A. Komarov, M. Salhi, A. Haboucha and F. Sanchez, J. Opt. A **8**, 319 (2006).

[6] D. Turaev, A.G. Vladimirov, S. Zelik, Phys. Rev. E **75**, 045601(R) (2007).

[7] J.-M. Soto-Crespo, Ph. Grelu, N. Akhmediev, N. Devine, Phys. Rev. E **75** 016613 (2007).

[8] A. Zavyalov, R. Iliew, O. Egorov, F. Lederer, Phys. Rev A **79**, 053841 (2009).

[9] A.G. Vladimirov, G.V. Khodova, N.N. Rosanov, Phys. Rev. E, **63**, 056607 (2001).

[10] N.N. Rosanov, *Spatial Hysteresis and Optical Patterns*, (Springer, Berlin, 2002).

[11] H. Vahed, R. Kheradmand, H. Tajalli, G. Tissoni, L.A. Lugiato, and F. Prati, Phys. Rev. A **84**, 063814 (2011).

[12] D.Y. Tang, W.S. Man, H.Y. Tam, and P.D. Drummond, Phys. Rev. A **64**, 033814 (2001).

[13] Ph. Grelu, F. Belhache, F. Gutty, and J.-M. Soto-Crespo, Opt. Lett. **27**, 966 (2002); Ph. Grelu, J. Beal, and J.-M Soto-Crespo, Opt. Express **11**, 2238 (2003).

[14] Y. Tanguy, T. Ackemann, W. J. Firth and R. Jäger, Phys. Rev. Lett. **100**, 013907 (2008).

[15] N. Radwell and T. Ackemann, J. Quantum Electronics **45**, 1388 (2009); N. Radwell et al., Eur. Phys. J. D **59**, 121 (2010).

[16] P. Genevet, S. Barland, M. Giudici, and J.R. Tredicce, Phys. Rev. Lett. **101**, 123905 (2008).

[17] T. Elsass et al., App. Phys. B **98**, 327 (2010).

[18] P. Genevet, M. Turconi, S. Barland, M. Giudici, and J.R. Tredicce, Eur. Phys. J. D **59**, 109 (2010).

[19] R. Adler, Proc. IRE **34**, 351 (1946); reprinted in Proc. IEEE **61**, 1380 (1973).

[20] A. Pikovsky, M. Rosenblum, and J. Kurths *Synchronization. A universal concept in nonlinear sciences* (Cambridge University Press, Cambridge, 2001).

[21] C.J. Buczek, R.J. Freiberg, and M.L. Skolnick, Proc. IEEE **61**, 1411 (1973).

[22] L. Fabiny, P. Colet, R. Roy, and D. Lenstra, Phys. Rev. A **47**, 4287 (1993).

[23] P. Coullet, D. Daboussy, and J.R. Tredicce, Phys. Rev. E **58**, 5347 (1998).

[24] D. Goulding et al., Phys. Rev. Lett. **98**, 153903 (2007).

[25] J. Thevenin, M. Romanelli, M. Vallet, M. Brunel, and T. Erneux, Phys. Rev. Lett. **107**, 104101 (2011).

[26] A.J. Scroggie, W.J. Firth, and G.-L. Oppo, Phys. Rev. A **80**, 013829 (2009).

[27] P.V. Paulau, D. Gomila, P. Colet, B.A. Malomed, and W.J. Firth, Phys. Rev. E **84**, 036213 (2011).

[28] Y. He et al., Opt. Lett. **34**, 2976 (2009).

[29] W. Chang, N. Akhmediev, and S. Wabnitz, Phys. Rev. A **80**, 013815 (2009); W. Chang, N. Akhmediev, S. Wabnitz, and M. Taki, J. Opt. Soc. Am. B **26**, 2204 (2009).

[30] This follows the procedure used to control the detuning of coupled microchip lasers, e.g. [22], with additional coupled cavity effects.

[31] S. Wieczorek, B. Krauskopf, T. B. Simpson, and D. Lenstra, Phys. Rep. **416**, 1 (2005).

[32] D. Cumin and C.P. Unsworth, Physica D **226**, 181 (2007).